Supporting Information

Interfacial electronic modulation in electrochemical reconstructed $CoOOHCuO@CeO_2$ for efficient electrooxidation of 5-hydroxymethylfurfural

Haokun Pan,[a] Yifei Ye,[a] Yetong Liu,[a] Cheng Zhang,[b] Xiubing Huang*[a]

[a] Beijing Key Laboratory of Function Materials for Molecule & Structure Construction, School of Materials Science and Engineering, University of Science and Technology Beijing, Beijing 100083, P. R. China

[b] Baotou Research Institute of Rare Earths, Baotou 014030, P. R. China

*Corresponding authors: xiubinghuang@ustb.edu.cn (X. Huang)

Chemicals and Materials

All chemicals and materials were utilized exactly as received, with no further purification. Cobaltous nitrate hexahydrate [$Co(NO_3)_2 \cdot 6H_2O$, 99.99%] and Copper nitrate Trihydrate [$Cu(NO_3)_2 \cdot 3H_2O$, 99.9%] was purchased from AI LAN (Shanghai) Chemical Technology Co., Ltd. N,N-Dimethylmethanamide [DMF, AR] was purchased from Beijing Tongguang Fine Chemical Co., Ltd. Cerium(III) nitrate hexahydrate [$Ce(NO_3)_3 \cdot 6H_2O$, 99.5%] was purchased from Thermo Fisher Scientific (China) Co., Ltd. 5-Hydroxymethylfurfural [HMF, 99.54%], furan-2,5 dicarbaldehyde [DFF, 98%] were purchased from Ark Pharma Scientific Co., Ltd. Potassium hydroxide [KOH, 95%], 5-hydroxymethyl-2-furancarboxylic acid [HMFCA, 98%], 5-formyl-2 furancarboxylic acid [FFCA, >98%], 2,5-furandicarboxylic acid [FDCA, 98%] were purchased from Shanghai Aladdin Bio-Chem Technology Co., Ltd. Hydrophilic Carbon Cloth (CC, 0.36 mm) was purchased from Zancheng (Tianjin) Technology Co., Ltd.

Synthesis

Pretreatment of Carbon Cloth (CC):

Carbon cloth (CC) was cut into rectangular pieces with dimensions of 2 × 4 cm^2. An appropriate amount of acetone (sufficient to completely immerse the CC) was poured into a 100 mL beaker. The cut CC pieces were fully immersed in the acetone. The beaker was then placed in an ultrasonic cleaner for bath sonication for 15 min. After sonication, the acetone-treated CC was transferred to a beaker containing deionized (DI) water and subjected to another 15 min of bath sonication. Subsequently, the DI water was replaced with absolute ethanol, and the ultrasonic cleaning step was repeated for an additional 15 min.

Hydrothermal Synthesis of CC@$CoCu_x$-MOF:

The CC@$CoCu_x$-MOF was fabricated through a tailored hydrothermal protocol. Briefly, a homogeneous solvent mixture was first prepared by combining 32 mL of DMF, 2 mL of deionized water, and 2 mL of absolute ethanol under vigorous stirring. Into this mixture, (1.0 + x) mmol of terephthalic acid (H_2BDC) was introduced as the organic linker, and the solution was sonicated for 20 minutes to achieve complete dissolution. The metal precursors—1.0 mmol of cobalt nitrate hexahydrate and x mmol of copper nitrate trihydrate—were then sequentially added, followed by continuous magnetic stirring for 30 minutes to guarantee a homogeneous reaction cocktail. This final

precursor solution was transferred into a Teflon-lined autoclave, wherein a piece of pretreated carbon cloth (2 × 4 cm^2) was carefully positioned against the inner wall. The sealed reactor was subsequently subjected to a 48-hour hydrothermal treatment at 140 °C in a thermostatic oven. After natural cooling to ambient temperature, the resulting CC@$CoCu_x$-MOF was retrieved, meticulously rinsed with ethanol and DI water in triplicate, and ultimately vacuum-dried at 60 °C for 12 hours.

Electrodeposition Synthesis of CC@$CoCu_{0.5}$-MOF@CeO_2:

The decoration of CeO_2 onto the CC@$CoCu_{0.5}$-MOF scaffold was engineered via a controlled electrodeposition process. First, the CC@$CoCu_{0.5}$-MOF substrate was precisely sectioned into working electrodes, each with a defined geometric area of 1 cm^2. The electrodeposition bath was formulated by dissolving 0.868 g of cerium(III) nitrate hexahydrate and 0.5844 g of sodium chloride in 100 mL of deionized water. The deposition itself was conducted in a 70 °C oil bath to enhance ion mobility. During this step, the immersed electrode area was rigorously maintained at 1 cm^2, and a constant cathodic current density of 0.5 mA cm^{-2} was applied. A series of samples were synthesized with deposition times of 300, 600, 900, and 1200 seconds to probe the time-dependent morphology. For the sake of clarity and unless explicitly stated otherwise, the sample designated as CC@$CoCu_{0.5}$-MOF@CeO_2 in this work specifically corresponds to the one prepared with the 600-second electrodeposition protocol.

Characterizaiton

The morphology and microstructure were obtained by field emission scanning electron microscopy (FE-SEM, Hitachi SU8010, Japan) and transmission electron microscopy (TEM, JEM 2200FS, Japan). The X-ray diffraction (XRD) patterns were acquired through a Bruker D8 ADVANCE with Cu K_α radiation (λ = 1.5406 Å) at 40 kV and 40 mA. Analyses of surface chemical states were carried out on an X-ray photoelectron spectrometer (XPS) of Thermo Scientific K-Alpha (Al $K_{\alpha 1}$: 1486.6 eV), and all spectra were calibrated based on the C 1s peak (284.8 eV).

Electrochemical measurements

All electrochemical data were acquired using a CHI660D electrochemical workstation. The measurements employed a standard three-electrode configuration: a self-supporting electrode (1 cm × 1 cm), a graphite rod, and an Hg/HgO electrode served as the working electrode, counter electrode, and reference electrode, respectively. For the OER and HMFOR studies, the electrolytes were 1.0 M

KOH and 1.0 M KOH containing 50 mM HMF, respectively. To prevent the possible base-catalyzed degradation of HMF and the Cannizzaro reaction, the electrolyte used should be freshly prepared and used immediately to minimize any impact. Linear sweep voltammetry (LSV) curves were recorded at a deliberate scan rate of 5 mV s^{-1}. Tafel slopes were subsequently extracted by applying the Tafel equation to the strongly polarized segments of these LSV traces. Electrochemical impedance spectroscopy (EIS) probed the interfacial processes, with the frequency sweeping from 10^5 down to 10^{-2} Hz at a fixed amplitude of 5 mV. Critically, these EIS spectra were captured in-situ across a range of applied potentials, mapping the evolution of charge transfer dynamics. The double-layer capacitance (C_{dl}) and the electrochemical surface area (ECSA) were derived from a series of cyclic voltammetry (CV) scans. The electrochemical activation was performed via CV in 1.0 M KOH within the potential range of 0.925–1.725 V vs. RHE at a scan rate of 50 mV s^{-1} for 50 cycles, which ensured complete reconstruction of CoCu-MOF to CoOOHCuO. C_{dl} was calculated from CVs in the non-Faradaic region (0.684–0.784 V vs. RHE) at scan rates of 20–100 mV s^{-1}. For all linear sweep voltammetry (LSV) data presented, iR-correction was routinely applied unless otherwise noted, utilizing the relationship Ecorrected= Emeasured- iRs. Here, the uncompensated solution resistance (Rs) was directly extracted from the high-frequency intercept of the corresponding electrochemical impedance spectroscopy (EIS) measurement. Furthermore, all reported potentials were converted to the reversible hydrogen electrode (RHE) scale to ensure consistent benchmarking, achieved through the conversion formula: E (vs. RHE) = E (vs. Hg/HgO) + 0.0591 × pH + 0.098.

2.5. High performance liquid chromatography analysis

The identification and quantification of the substrate (HMF), intermediates (HMFCA, FFCA, and DFF), and the final oxidation product (FDCA) were performed by high-performance liquid chromatography (HPLC, Agilent 1260 Infinity Series, USA) coupled with an ultraviolet-visible (UV-Vis) detector and an Agilent Zorbax SB-C18 column (150 mm × 4.6 mm, 5 μm). A mixture of 5 mM ammonium formate and methanol, with a volume ratio set at 7:3, was employed as the mobile phase. The chromatographic separation was governed by a fixed set of parameters: a flow rate of 0.6 mL min^{-1}, a column temperature maintained at 30 °C, and a separation time of 10 min. To quantify the HMFOR products, the electrocatalytic reaction was first performed in an 8 mL electrolyte comprising 1.0 M KOH and 10 mM HMF. Once a pre-defined charge had passed at the fixed potential of 1.4

VRHE, the process was paused. A 50 μL aliquot was then immediately withdrawn from the reaction mixture, subjected to a 100-fold dilution with 5 mL of H_2O, and finally injected into the HPLC for precise analysis. The carbon recovery rate of the final products was quantitatively analyzed using the initial HMF (at 0 C) as the reference standard. The conversion of HMF was subsequently quantified using the following relationship:

$$\text{HMF conversion} = \frac{\text{mole of consumed HMF}}{\text{mole of initial HMF}} \times 100\%$$

Product selectivity was calculated by the equation.

$$\text{Selectivity} = \frac{\text{mole of certain product}}{\text{mole of all the detected products}} \times 100\%$$

FE of FDCA production was calculated by the equation.

$$\text{FE(FDCA)} = \frac{\text{mole of produced product}}{\text{total charge passed}/(6 \times \text{F})} \times 100\%$$

where F is the Faraday constant (96485 C mol^{-1}).

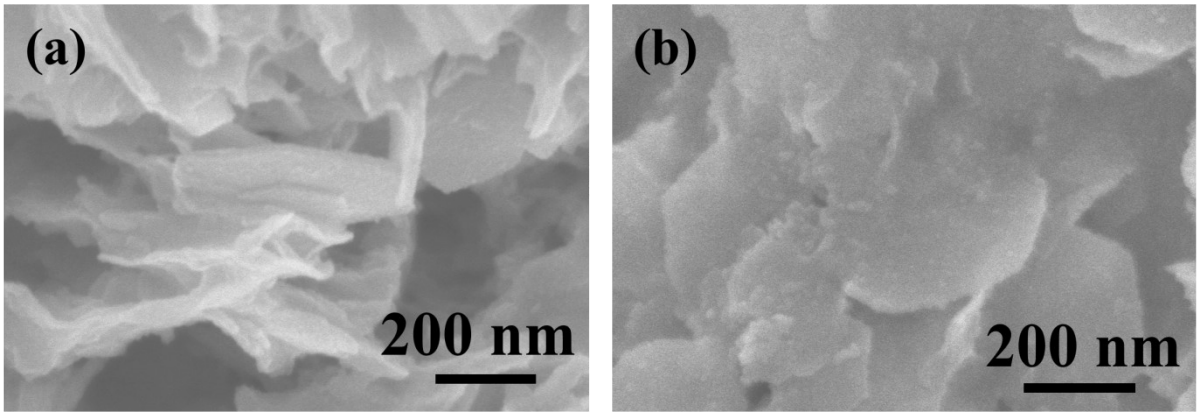

Figure S1. SEM image of (a) CC@$CoCu_{0.5}$-MOF and (b) CC@$CoCu_{0.5}$-MOF@CeO_2.

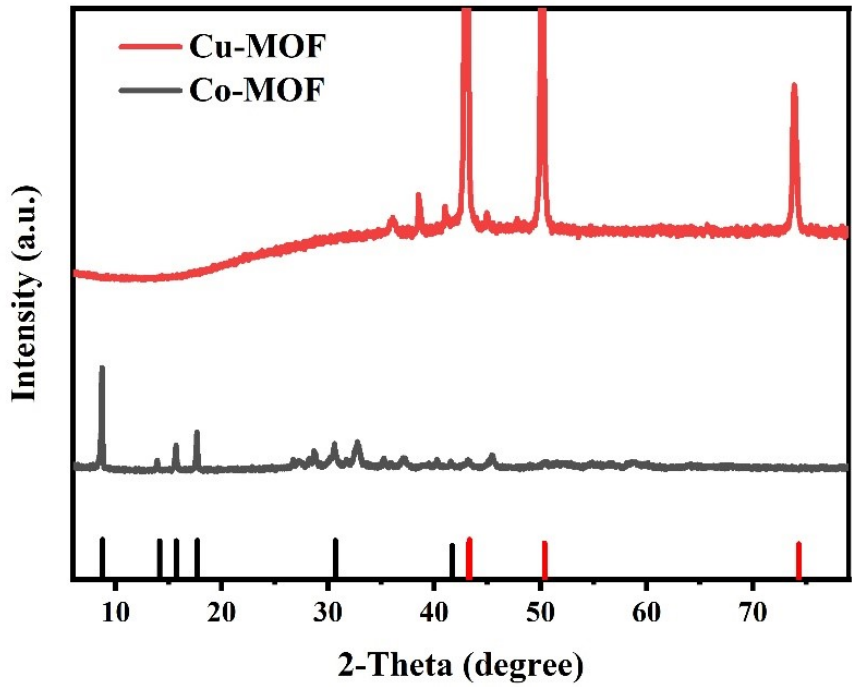

Figure S2. XRD patterns of CC@Co-MOF and CC@Cu-MOF.

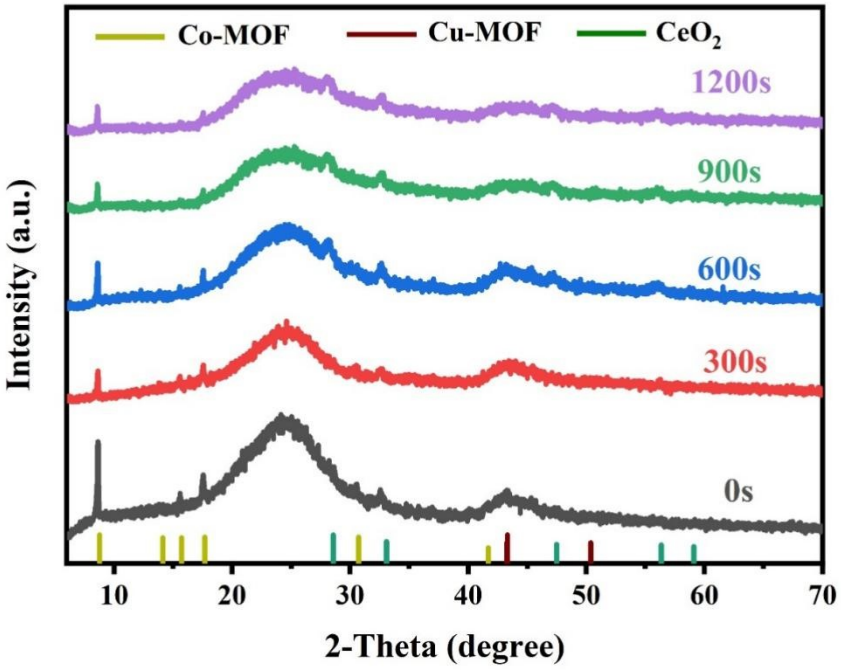

Figure S3. XRD patterns of CC@$CoCu_{0.5}$-MOF@CeO_2 at different electrodeposition times.

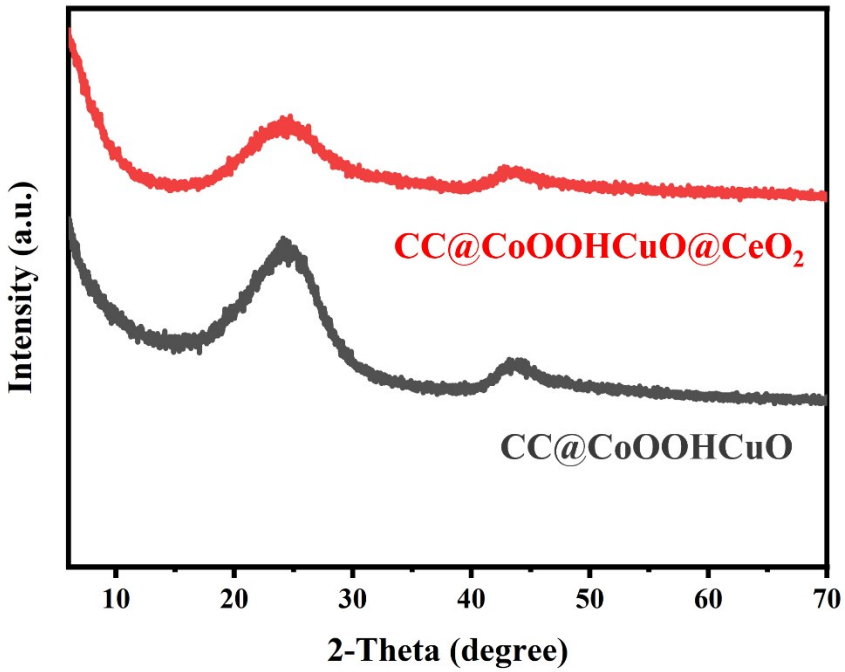

Figure S4. XRD patterns of CC@CoOOHCuO and CC@CoOOHCuO@CeO_2 after CV action.

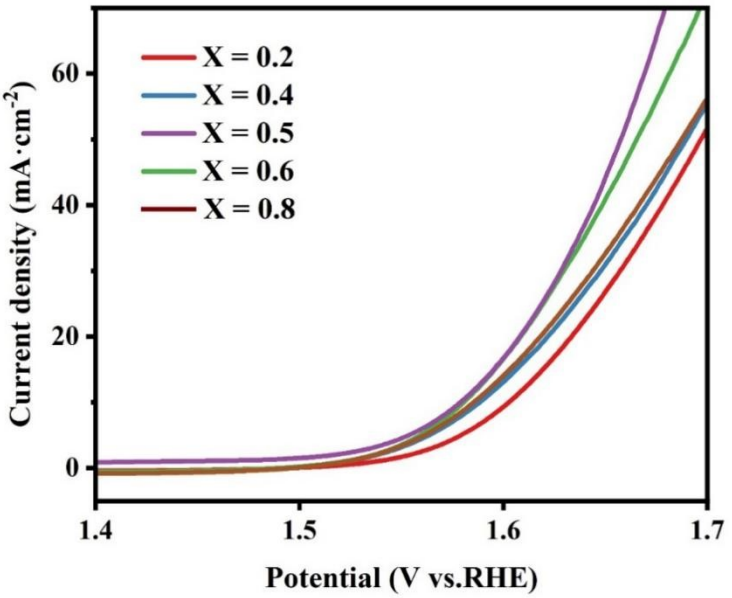

Figure S5. The LSV curves of CC@CoCu$_x$-MOF@CeO$_2$ (after CV action) with different X values.

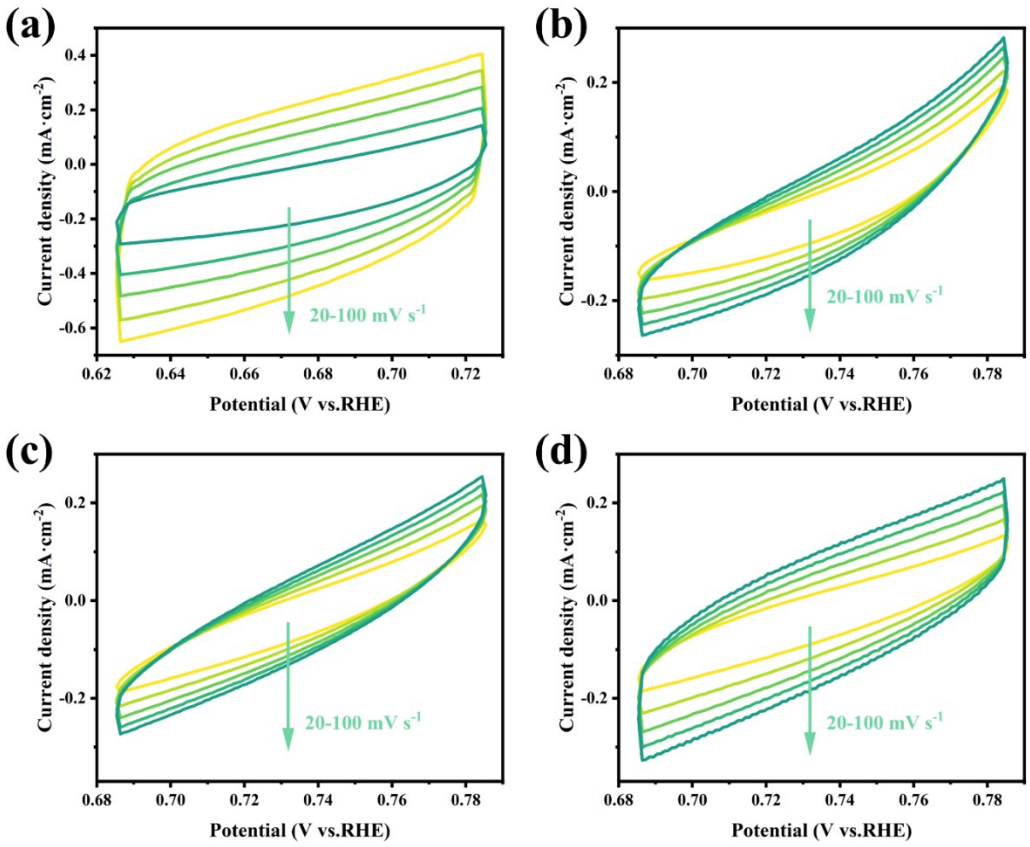

Figure S6. CV curves at 100, 80, 60, 40 and 20 mV s^{-1} for (a) CC@CuO, (b) CC@CoOOH, (c) CC@CoOOHCuO, and (d) CC@CoOOHCuO@CeO$_2$.

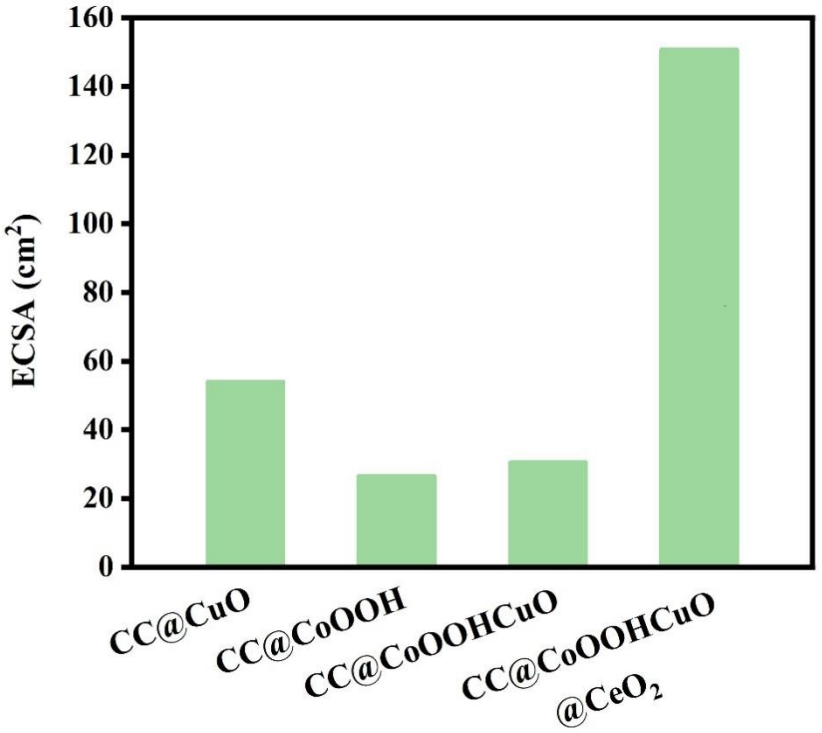

Figure S7. ECSAs of CC@CuO, CC@CoOOH, CC@CoOOHCuO, and CC@CoOOHCuO@CeO_2.

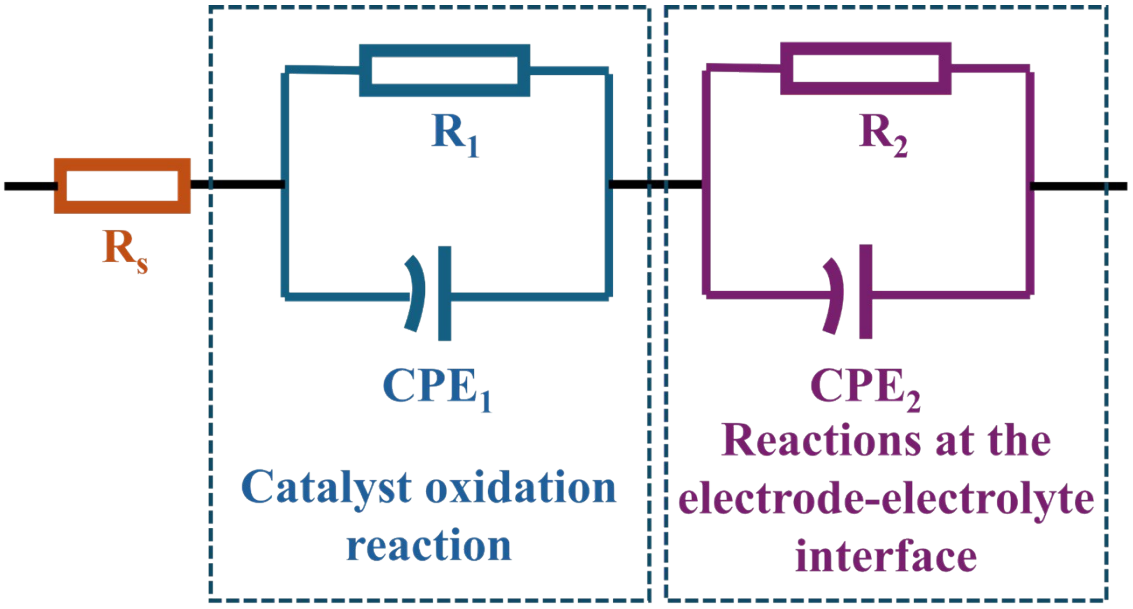

Figure S8. The equivalent circuit for fitting EIS spectra.

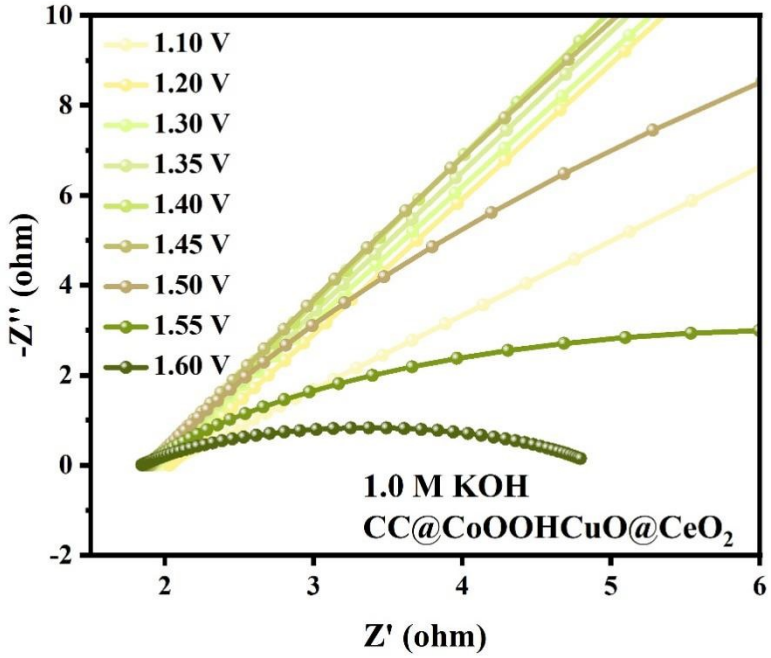

Figure S9. Nyquist plots of CC@CoOOHCuO@CeO_2 in 1.0 M KOH.

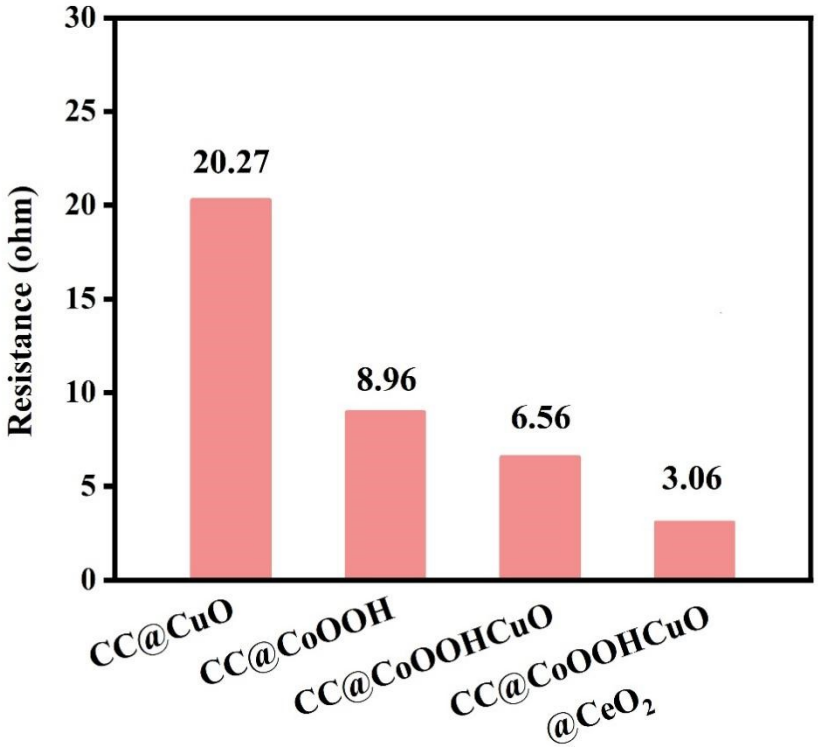

Figure S10. R_{ct} values of for CC@CuO, CC@CoOOH, CC@CoOOHCuO, and CC@CoOOHCuO@CeO_2 OER at 1.55 V_{RHE} in 1.0 M KOH.

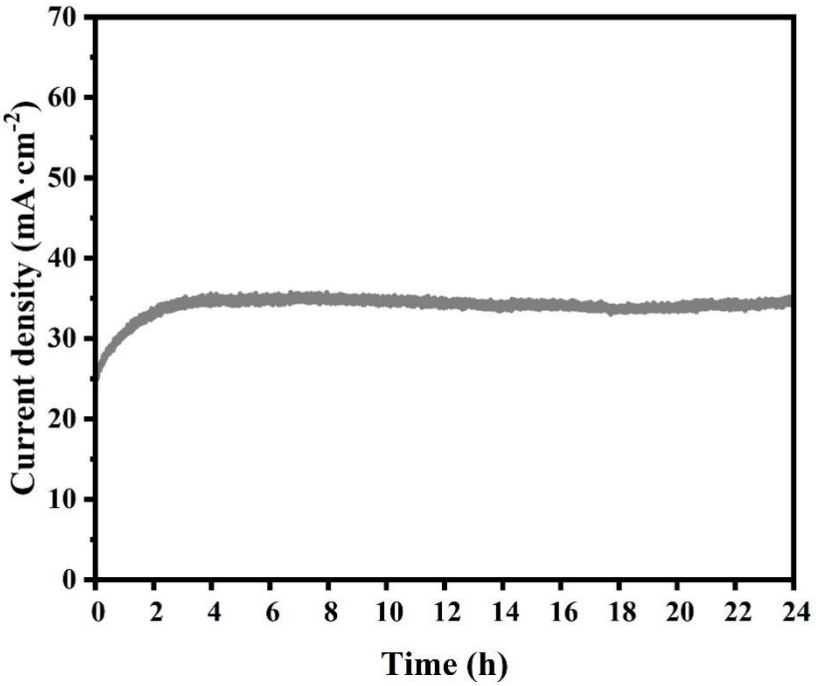

Figure S11. Current density-time curve of CC@CoOOHCuO@CeO_2 in 1.0 M KOH.

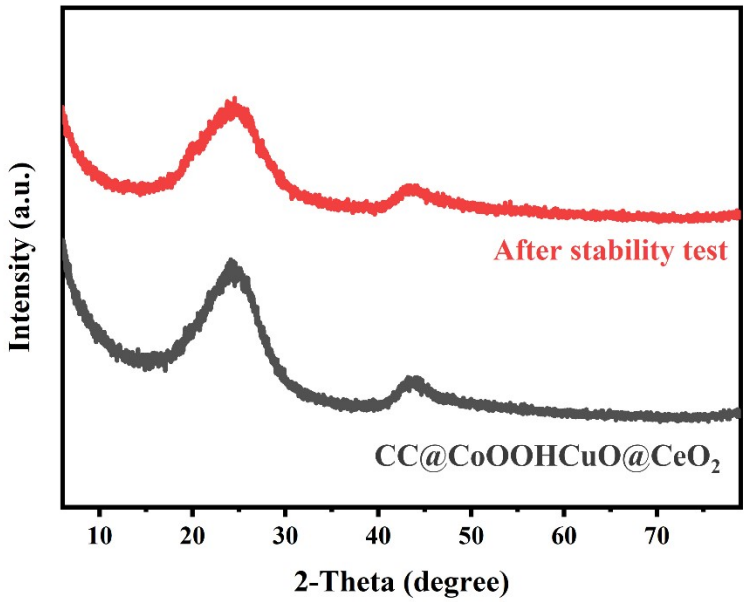

Figure S12. XRD patterns of CC@CoOOHCuO@CeO_2 before and after stability test.

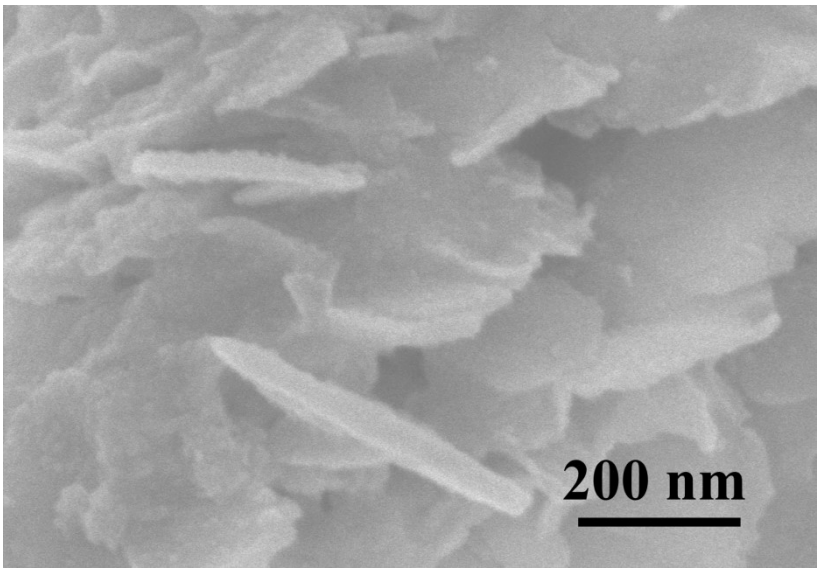

Figure S13. SEM image of CC@CoOOHCuO@CeO_2 before and after stability test.

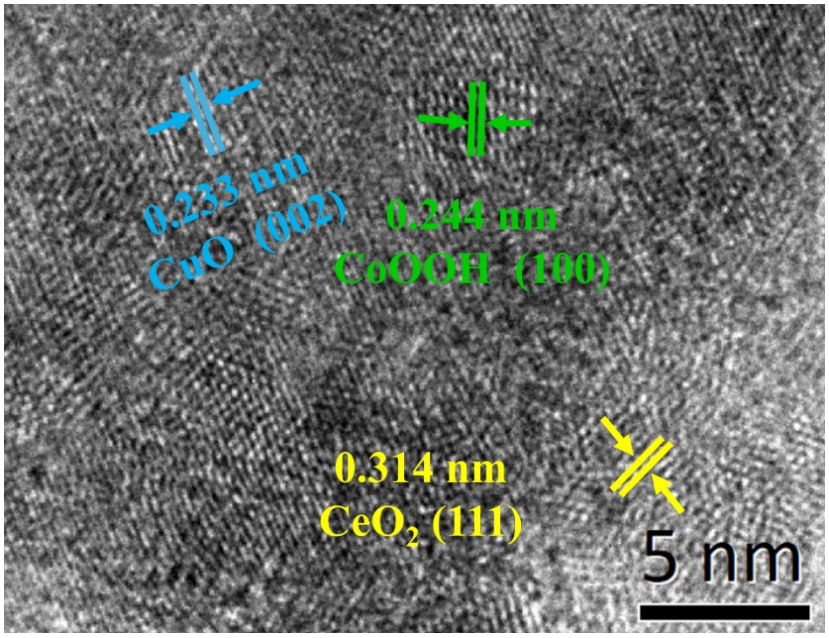

Figure S14. HRETM image of CC@CoOOHCuO@CeO_2 after stability test.

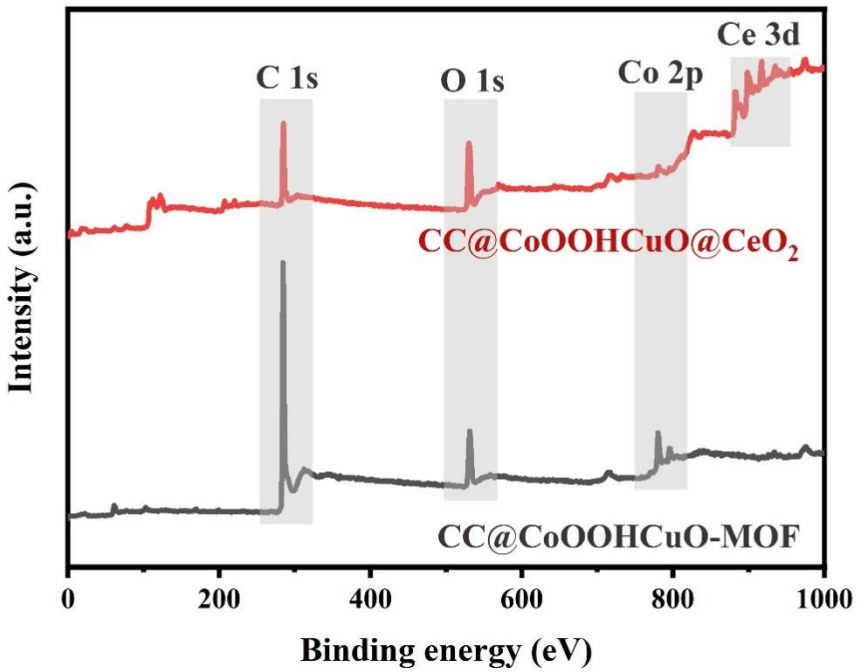

Figure S15. Survey XPS spectra of CC@CoOOHCuO and CC@COOHCuO@CeO_2.

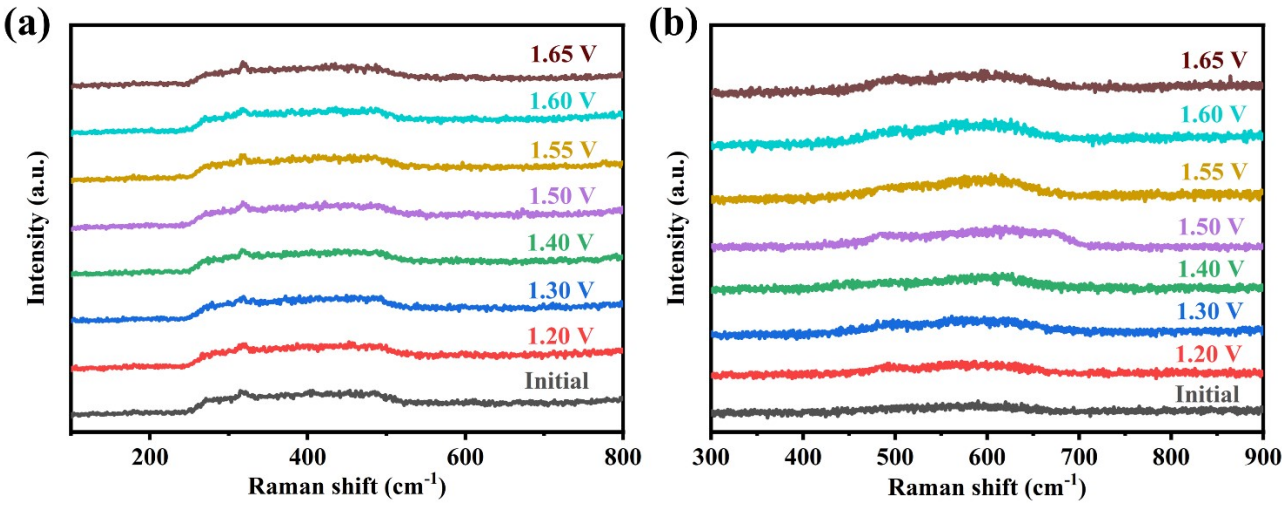

Figure S16. In-situ Raman spectra of (a) CC@CoOOHCuO and (b) CC@CoOOHCuO@CeO_2 at different applied potentials.

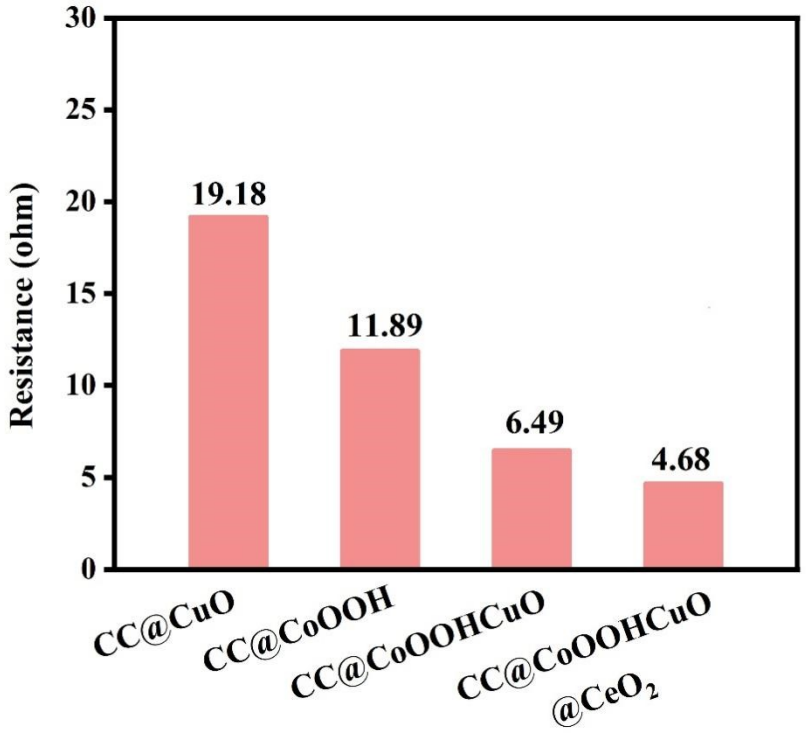

Figure S17. R_{ct} values of for CC@CuO, CC@CoOOH, CC@CoOOHCuO, and CC@CoOOHCuO@CeO_2 HMFOR at 1.55 V_{RHE} in 1.0 M KOH + 10 mM HMF.

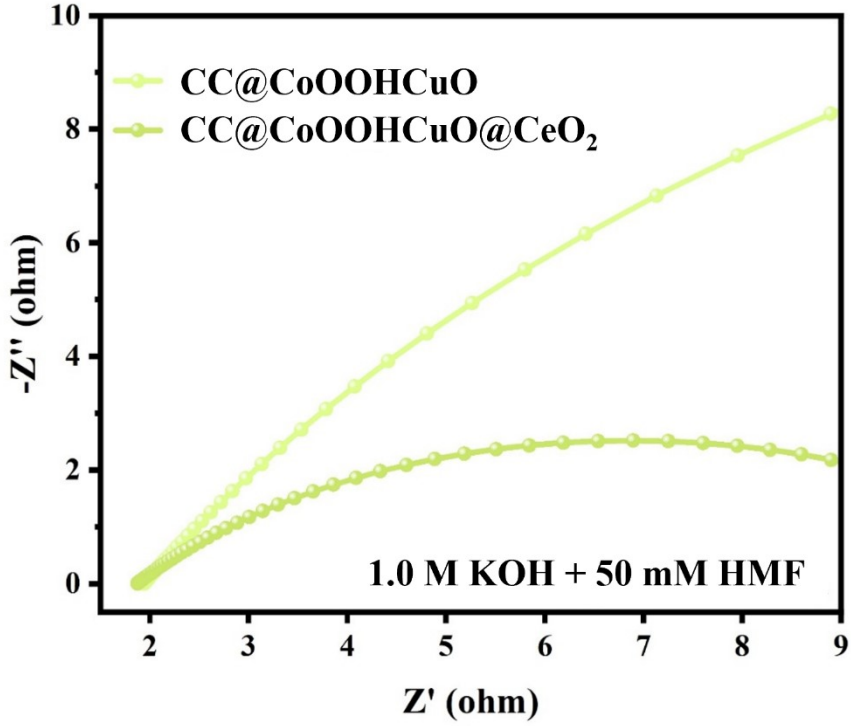

Figure S18. EIS spectra of CC@CoOOHCuO and CC@CoOOHCuO@CeO_2 at 1.45 V_{RHE} in 1.0 M KOH + 10 mM HMF.

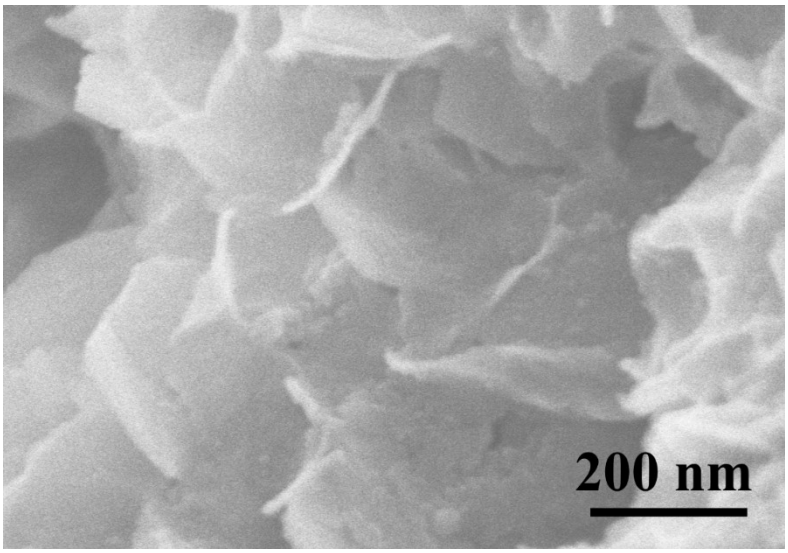

Figure S19. SEM image of CC@CoOOHCuO@CeO_2 after HMFOR cyclic stability test.

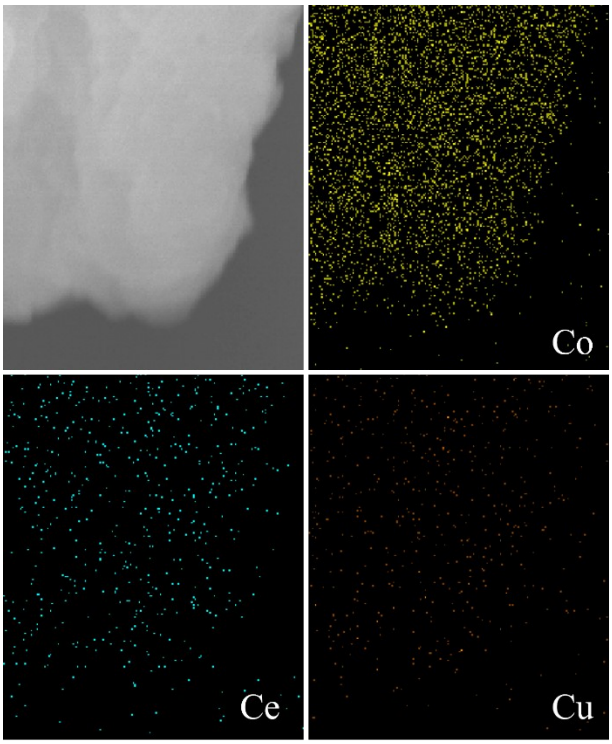

Figure S20. EDS image of CC@CoOOHCuO@CeO_2 before and after stability test.

Table S1. The system resistance (R_s) calculated from EIS data (OER at 1.55 V_{RHE}, 1.0 M KOH).

Samples	R_s (Ω)
CC@CuO	2.561
CC@CoOOH	2.521
CC@CoOOHCuO	2.493
CC@CoOOHCuO@CeO_2	2.449

Table S2. The system resistance (R_s) calculated from EIS data (HMFOR at 1.40 V_{RHE}, 1.0 M KOH + 50 mM HMF).

Samples	R_s (Ω)
CC@CuO	1.941
CC@CoOOH	1.904
CC@CoOOHCuO	1.871
CC@CoOOHCuO@CeO_2	1.863

Table S3. Summary of HMFOR performance of some reported catalysts in alkaline media.

Catalyst	Electrolyte composition	Potential (V_{RHE})	Product	FE (%)	Ref.
CC@CoOOHCuO@CeO_2	1 M KOH + 10 mM HMF	1.40	FDCA	96.3	This work
Mn_3O_4/CeO_2	1 M KOH + 10 mM HMF	1.63	FDCA	93.9	1
NiS_x/Ni_2P	1 M KOH + 10 mM HMF	1.25	FDCA	95.1	2
Ni/Co	1 M KOH + 10 mM HMF	1.45	FDCA	92.1	3
Co_3O_4	1 M KOH + 10 mM HMF	1.65	FDCA	92.9	4
Y-Co-CoS_x@CN	0.1 M KOH + 5 mM HMF	1.40	FDCA	93.5	5
NiCoFeS-MOF	1 M KOH + 50 mM HMF	1.39	FDCA	99	6
CoFe PBA	1 M KOH + 10 mM HMF	1.42	FDCA	94	7
Cr-$Ni(OH)_2$/CC	1 M KOH + 10 mM HMF	1.47	FDCA	96	8
CoCu	1 M KOH + 50 mM HMF	1.40	FDCA	96	9
CoMoP	1 M KOH + 100 mM HMF	1.36	FDCA	93.3	10
Ni_1Mn_5-LDH	1 M KOH + 100 mM HMF	1.40	FDCA	97	11
NiCoFe-LDHs	1 M NaOH + 5 mM HMF	1.52	FDCA	90	12

NA: not available.

Table S4. The atomic percent of CC@CoOOHCuO@CeO_2 before and after stability test.

Atomic	Co (wt%)	Cu (wt %)	Ce (wt %)
Before stability test	27.08	18.28	30.15
After stability test	24.54	21.19	37.60

References

1. Y. Huang, H. Dai, Z. Huang, G. Wang, H. Zhao, X. Pang, W. Fan and H. Bai, *Chemical Engineering Journal*, 2024, **479**, 147779.
2. B. Zhang, H. Fu and T. Mu, *Green Chemistry*, 2022, **24**, 877-884.
3. S. Fan, B. Zhu, X. Yu, Y. Gao, W. Xie, Y. Yang, J. Zhang and C. Chen, *Journal of Energy Chemistry*, 2024, **92**, 1-7.
4. C. Chen, Z. Zhou, J. Liu, B. Zhu, H. Hu, Y. Yang, G. Chen, M. Gao and J. Zhang, *Applied Catalysis B: Environmental*, 2022, **307**, 121209.
5. J. Chen, Y. Wang, M. Zhou and Y. Li, *Chemical Science*, 2022, **13**, 4647-4653.
6. Y. Feng, K. Yang, R. L. Smith and X. Qi, *Journal of Materials Chemistry A*, 2023, **11**, 6375-6383.
7. W. Hadinata Lie, C. Deng, Y. Yang, C. Tsounis, K.-H. Wu, M. V. Chandra Hioe, N. M. Bedford and D.-W. Wang, *Green Chemistry*, 2021, **23**, 4333-4337.
8. Z. Yang, B. Zhang, C. Yan, Z. Xue and T. Mu, *Applied Catalysis B: Environmental*, 2023, **330**, 122590.
9. Y. Zhu, J. Shi, Y. Li, Y. Lu, B. Zhou, S. Wang and Y. Zou, *Journal of Energy Chemistry*, 2022, **74**, 85-90.
10. H. Wang, C. Niu, W. Liu and S. Tao, *Applied Catalysis B: Environmental*, 2024, **340**, 123249.
11. Y.-R. Bao, Y. Duan and Y. Na, *Journal of Materials Chemistry A*, 2023, **11**, 18668-18671.
12. M. Zhang, Y. Liu, B. Liu, Z. Chen, H. Xu and K. Yan, *ACS Catalysis*, 2020, **10**, 5179−5189.